# Non-rigid registration method to assess breath holding reproducibility with ABC in lung cancer treatment

D. Sarrut, V. Boldea and ...

*Abstract*—

*Purpose:* **To study the interfraction reproducibility of breath holding using active breathing control (ABC) device. To develop computerized tools to evaluate 3D intra-thoracic motion adapted to each patient.**

*Methods and materials:* **Since June 2002, 11 patients with non-small cell lung cancer (NSCLC) were enrolled in a phase II trial. For each patient one CT scan was acquired during free-breathing (reference) and three CT scans were acquired using the ABC device. Patients were breath held at the same preselected phase in the breathing cycle (about 70% of the vital capacity). Patients were then treated with 3D-conformal radiotherapy and with ABC device. The prescribed dose was 70 Gy, adapted to the lung DVH. We develop automated computerized tools to:**

**a) Perform volumes comparisons. Lungs volumes were evaluated with an automated 3D segmentation algorithm.**

**b) Analyze lung interfraction deformation with 3D non-rigid registration. All the CT scans of a patient were first put in a same reference frame by an intensity based rigid registration algorithm. Then, we performed an iterative non-rigid registration algorithm. It leads to a dense 3D vector field displacement vector for each point in lung volume. In order to obtain a measure of pure deformation (without taking into account setup displacement), rigid transformation was subtracted from both vector fields and points displacements.**

*Results:* **All patients, except one, have been treated with ABC during 7 weeks without any problem. On the 8 available datasets, we distinguished two kind of results. For 6 patients, lung volume differences are below 5% and mean (standard deviation) of intra-pulmonary 3D displacements are between 2.3(1.4) and $4\,mm(3.3)$, slightly greater in the inferior part of the lung than in the superior part. For two patients, we detected changes in volume greater than $300\,cc$ and displacement greater than $10\,mm$.**

*Conclusion:* **For 6 patients, hold breathing with ABC is effective. The two other patients have clinical reasons to explain discrepancies (atelectasia and emphysema). The proposed 3D non-rigid registration method allows to perform personalized evaluation of breath hold reproducibility with ABC, and will then be used to adapt patient-specific internal margin.**

*Keywords*— **keyword keyword keyword keyword**

## I. INTRODUCTION

Organ motion due to respiratory cycle is known to be a source of inaccuracy in the treatment delivery because it leads to tumor displacement and suboptimal dose delivery. Imaging studies using fluoroscopy have shown that tumors and organs can move from $10\,mm$ to more than $30\,mm$ (for diaphragm) during the breathing cycle [1], [2]. A main challenge non small-cell lung cancer (NSCLC) radiotherapy is the ability to spare surrounding normal tissues while providing prescribed dose to the tumor, because *1)* dose escalation seems to yield superior outcomes [3], [4], [5] and *2)* normal lung tissue is very sensitive to radiation: Tsujino et al. [6], [7] correlate the risk of developing severe pneumonitis to the volume of irradiated lung.

Taking into account organ motion is studied with several approaches. The most common/simple approaches consist in adapting internal margins (defined in the ICRU Report 62) [8], [9], [10], [11]. A drawback of such techniques is they relied on averaged, predictable, regular, reproducible organs and tumor motion models, while numerous studies show that lung tumor motion remains more complex than a simple cyclic pathway [5], [12], [13], [14], [15], [16], [17].

Another promising/ambitious approach is synchronizing the radiation delivery with patient's breathing: treatment beam is activated at predetermined range in the breathing cycle while patient (shallow) breath freely [18], [19], [11], [17], [12]. The drawbacks are they could require invasive placement of internal fiducial markers, or they relied on a correlation between external and internal movement, which is not yet well established [12].

We are interested here in a intermediate approach: immobilizing the organs by breath holding (BH). Intrafraction motion occurs during the delivery of radiation treatment, during a BH. Interfraction motion is the change or displacement of the tumor from one day to the next. Measured movements during a BH phase is considered as negligible ( $1mm$) with active BH [20], [21], [22], and evaluated between 1.0 and $1.8\,mm$ for self BH [18], [8], [23]. The interfraction reproducibility of NE/NI BH tend to be better than DIBH for some authors [24], [20] also inverse tendance have been reported [25]. However, DIBH has also the ability to increase lung volume in order to decrease the mass of irradiated lung.

The goal of this study is develop a non-rigid 3D registration method to systematically evaluate the interfraction reproducibility of BH with Active Breath Control device (ABC). Such approach allows to estimate the 3D displacement of each point between different CT scan and thus help determining adapted internal margins. In the following we use the following abbreviations: FB (free breathing), BH (breath holding), NI (end of normal inspiration), NE (end of normal expiration), DI (deep inspiration), DE (deep expiration).

## II. MATERIAL AND METHOD

### A. Data acquisition

#### A.1 Patients

Since June 2002, 11 patients with non-small cell lung cancer (NSCLC) were enrolled in a phase II trial. Radical radiotherapy was indicated because they all have potentially resectable but inoperable T1-T4, N0-N1, M0 NSCLC. Patients have all severe respiratory insufficiency. For all patients, informed consent was obtained in accordance with the procedures of the French CCPPRB[1].

#### A.2 Active breath holding

ABC (Active Breathing Control) was proposed by Wong et al. [1] as a device allowing temporary immobilization of respiratory motion by implementing a BH at a predefined relative lung volume and air flow direction. At a preset lung volume during either inspiration or expiration, airflow of the patient is temporarily blocked, thereby immobilizing breathing motion. The duration of the active BH is set such that the patient can comfortably maintained it. Radiation will be turned on and off during this period. At our knowledge, several studies report use of ABC for liver [20], breast [22], [26], [27], [28], [29], [30] and lung cancer [1], [31], [21], [4].

#### A.3 Patient breath holding with ABC

We use 2 ABC devices from Elekta (called *Active Breathing Coordinator*), one in the treatment room, the other in the scan room. The two devices were calibrated with a 2-L syringe. ABC allows to hold the breath at a predefined level relatively to the end of normal expiration (i.e. the functional residual capacity). Patients were breath held at the same preselected phase in the breathing cycle, in mDIBH, at about 70%/75% of the vital capacity depending on the patient ability. Patient follow a initial training session, during about XXX minutes, in order to find the maximum gate times they could reach in a relatively comfortable way (because they have to reproduce it as many times as the total number of fractions). BH duration was fixed between 15-20 sec regarding on patient ability. Verbal instructions was used during all BH sessions. BH session additional time is about XXX minutes for a treatment session.

#### A.4 CT scans

For each patient one CT scan was acquired during free-breathing (FB) (reference) and three CT scans were acquired in breath-hold (BH) using the ABC device. FB scans are acquired at the speed of an average respiratory cycle, about 4 sec [5]. BH scans were acquired in several breath hold sessions (range from X to Y sec according to the patient ability), like [4]. Slices (5mm thickness) are then stacked in a single 3D volume. Consistency between consecutive slices acquisitions was checked by visual inspection. Acquisition session time is about XXX minutes. The time between the three acquisitions range from 2 hours to several days (patient leaves the room between each session), allowing interfraction comparisons. Final 3D datasets sizes range are $512 \times 512$ with $[60-70]$ slices. 8 dataset (over 11) are available, leading to 24 CT scans acquired with ABC and 8 without.

#### A.5 Treatment

Patients were then treated with 3D-conformal radiotherapy and with ABC device. Contention is performed by $\alpha$-cradle [22]. The prescribed dose was 70 Gy, adapted to the lung DVH. Number of sessions range from XXX to YYY, with XXX fractions, leading to ZZZ breath holding with ABC.

### B. Lung volumes comparison

Our first goal was to develop a tool which allow to automatically quantify (left/right/whole) lung volumes in a reproducible way. The first step consists in segmenting whole lung with simple thresholding technique, such as [1], [31], [21]. Voxels with density below a fixed threshold are selected. Such voxels correspond to the air (outside and inside the patient), the lung and some gas (in the bowel for example). Then, the resulting binary image is labeled with a automated 3D connected components labeling algorithm (voxels neighborhood is chosen as 26-adjacency). Finally, only one connected component corresponding to the whole lung is automated selected (such component is the second largest ones, the first one being the air outside the patient).

Such technique does not require any user intervention, except setting the threshold. Measured lung volume is highly dependent on the chosen threshold (for example, it defines what part of the airways should be included in the lung volume). The choice of an "optimal" threshold is not very relevant for our problematic because we want to *compare* volume over the three CT of the same patient and, moreover, it is not clear such an "optimal" value exists. Hence, rather than using a single fixed threshold we choose to compare several lung volume measurements obtained from a range of 10 threshold values (between $-200$ and $-600$ HU), centered near an automated threshold, computed by the technique described in [32]. It leads to $8(patients) \times 3(CT) \times 10(threshold) = 240$ segmentations. In the following we denote LVD the Lung Volume Difference between 2 CT scans of a same patient.

#### B.1 Segmentation variability analysis

Our first study is to evaluate the influence of the threshold on the LVD. We first investigate the relation between threshold and lung volume according to the three CT of each patient. Range of threshold is chosen such that the relation is quasi linear. Slope of this linear relationship and extrema values of lung volumes are computed and compared.

[1] Comité Consultatif de Protection des Personnes dans la Recherche Biomédicale.

B.2 Lung volume difference analysis

For each patient, LVD between the each pair of the 3 CT are computed for each threshold. Differences are expressed in *cc* and in percentage of the first lung volume. When LVD are greater than XXX, we investigate the repartition of this difference between the left and the right lung. Lung separation is done with simple morphological tools. First, previously computed lung volume is progressively eroded (by a fixed number of erosion of 1 voxel kernel radius) in order to break the junction between the two lungs. Then, 3D connected components labeling is performed, and the two larger components remaining are labeled as right and left lung. Finally, these two components are dilated inside the initial whole lung volume in order to propagate the left and right labels. Trachea is also segmented using a similar technique. Mean lung density is also computed on each CT scan.

The goal is not to perform a perfect segmentation but to develop an automated and reproducible one which allows to compare volumes on a same basis. Figure 1 shows an example of the segmentation result.

*C. Motion estimation with non-rigid registration algorithm*

The goal is to estimate 3D displacement of individual lung points between two different acquisitions using image registration methods. Registering two images is finding a transformation which will pair as best as possible each point in one image (called reference image, denoted by $I$) with its correspondent in the second one (called object image, denoted by $J$) [33]. There are two main classes of transformations (denoted by $T$): rigid (translations, rotations) and non-rigid (allowing deformation). The complexity of the lung motion can not be reduced to a simple rigid transformation, so we used a 3D non-rigid registration method in order to be able to estimate local deformations between CT acquisitions.

Non-rigid methods can be classified into 2 categories: sparse vector field methods and dense vector fields methods. A sparse vector field method needs a set of control points (or landmarks) in the reference image with known correspondences in the object image. The final transformation is then computed by using a deformation model (such as thin-plate spline [34]) to interpolate the displacements of these points. However, correspondences between points of two different acquisitions are difficult to define or detect for lung, and final result highly depend on the accuracy of such corresponding points. Dense vector field methods compute a displacement vector in each point of the volume leading to potentially more robust points correspondence ; there is no need of control points.

We have use a home-made method based on the algorithm proposed by Thirion and Cachier [35], [36], [37]. The method, see [38], is a modified version of the optical flow technique [39] allowing to retreive large and small displacements. It is an iterative intensity based method, using image intensities (grey-levels) as features without requiring a segmentation step. Each iteration has two steps: pairing and regularising. *(1)* Corresponding point of $\boldsymbol{x}$ at iteration $i$, denoted by $u_i(\boldsymbol{x})$, is estimated according to local gradient of the reference image (eq 1, $J \circ T$ denotes the composition, $\nabla$ denotes the gradient operator, $\alpha$ is a parameter). Such method rely on the assumption of a grey level intensity conservation between two acquisitions (the two images are acquired with the same protocol). *(2)* The regularisation step consists in avoiding spatial inchoerences (for example two neighboring points with opposite motion). We use a 3D Gaussian recursive filter [40], which was shown to be close (under some assumptions) of a fluid regularisation [41].

$$u_i(\boldsymbol{x}) = \frac{I(\boldsymbol{x}) - J \circ T_{i-1}(\boldsymbol{x})}{\| \nabla I \|^2 + \alpha^2 (I(\boldsymbol{x}) - J \circ T_{i-1}(\boldsymbol{x}))^2} \nabla I \qquad (1)$$

This method result in a dense 3D deformation field, computed every $2\,mm$ in the in-plane dimension, between two scans: at each voxel of the first CT scan, a 3D vector is found, indicating where is the corresponding voxel in the second CT scan.

C.1 Residual error

The resulting deformation field is composed of two parts: a global rigid deformation (which corresponds to the missalignement of the patient between the two different acquisitions) and a part which is due to lung motion differences between two different breath holds. We called the latter the residual error. To find this residual error, we applied a 3D rigid registration algorithm [42], [43]. We adapted the algorithm in order to privilege the registration of the bonny rigid structures. Accuracy was verified by visual checking. Residual error is then obtained by substracting this rigid transformation from the deformation field obtained by non-rigid registration.

C.2 Data computation

Each CT acquisition is alternatively object and reference image. For each patient, we so computed 6 rigid and 6 non-rigid registrations, leading to 48 rigid and 48 non-rigid registrations. A vector fields represents $256 \times 256 \times 70 = 4.6$ millions of vectors, leading to about $52.5Mb$ (each vector is described with 4 bytes by coordinate). There are from 870 000 to 2 millions vectors in the lung according to the patient. We also divided the lung volume into 6 inferior-to-superior regions (superior 10%, 4 intermediate 20% regions, and inferior 10%) as described in [22] for results comparisons.

C.3 Visualisation

Dense 3D vector fields are difficult to visualise because of the amount of information. We have generate three kinds of images for a better visualisation and interpretation of the residual error. Figure 3 presents projected 3D vector field on a sagital, cranio-caudal and axial slice. Arrows correspond to residual error between two differents breath-holds, showing the displacement of the surrounding point. Density windowing of the slices was adapted for visual purpose in order to observe both low (inside lung) and high density points (rigid structures). Such 2D projection of the vector

field we don't have the third dimension of the information: the normal displacement of the projected vector. The same axial slice is depicted in figure 5 with a color depicting the cranio-caudal displacement. Green colors corresponds to displacements in the patient's head direction and blue colors corresponds to patient's foot direction. Green and blue intensities are scaled in function of the norm of the CC displacement Figure 6 illustrates the norm of the displacement vectors (dark red are small displacements, and light red are larger displacements).

## III. RESULTS

### A. Lung volume

#### A.1 Segmentation variability analysis

Lung volume is quasi-linear according to the threshold (mean of asymptotic standard errors lower than 0.3%). Relation between threshold and volume was found to remains quasi-constant between the 3 CT of each patient (difference between extrema volumes are lower than 60*cc* or 4%), but different from one patient to the other (the slop of the linear relationship between threshold and volume range from 1.1 to 2.0).

LVD according to different threshold are very consistent: for each patient, standard deviation (over the 10 segmentations) between LVD (expressed in percentage of the first volume) varies from 0.1 to 1.2%, meaning that LVD remains quasi-constant according to the the considered range of thresholds.

#### A.2 Lung volume difference analysis

LVD range from 8*cc* (0.2%) to more than 1000*cc* ($> 16\%$) in one case. Table I shows LVD for each patient and for the 3 CT comparisons, in *cc* and in percentage (gray boxes depict differences greater than 7%). For 2 patients ($n°3, 4$), some differences are superior to 7%. Table II depicts LVD repartition in left and right lung.

The mean lung density is $-834\,(20.5)$ HU or $0.17\,(0.02)$ $g/cm^3$ for all the images using ABC, and $-673\,(0.3)$ HU or $0.33\,(0.15)$ $g/cm^3$ for scan in FB (numbers in parenthesis are standard deviation). See table III. The increase in lung volume due to the mDIBH range from 19.5% to 34.5% according to the patient ability to perform a deep inspiration and regarding his FEV1 (Forced Expiratory Volume in the first second).

### B. Lung deformation

Table IV shows for each patient, mean, median and standard deviation of the displacement of all the points in the lung. The table also indicates mean of the 5% of points having greater displacement. For each patient, each value in the table is computed according to a mean of the 6 vector fields (AB, BA, AC, CA, BC, CB). Figure 2 represents mean points displacements (in mm) for each patient, in the ML, AP, CC directions and the 3D norm. Table V represents mean points displacements in each 6 successive vertical lung regions, for left and right lung. + SURFACE / VOLUME

## IV. DISCUSSION

### A. Compliance / patient tolerance

Among 11 patients with severe insufficiency respiratory, 1 was excluded and was not able to follow the treatment with ABC, due to inability to understand the procedure. Other patients have been treated daily with 35 fractions, leadings to more than 350XXX? BH with ABC. Additional time for each session is between 5 and 10 min, leading to a treatment time of about XXX min. This is coherent with other reports such as [20] (extra time about 10 min), or [22] which report a treatment duration inferior to 20 min. We use preselected phase in the breathing cycle of 70% of the vital capacity, which correspond to a medium DIBH (mDIBH) [22] ([1] use 80%, [22], [21] use 75%). BH time is about 20 sec, such as in [1], [20], [21], [4] (except for some patients with BH time of 30 to 45 sec for Hodgkin's cancer in [31], [1]) or liver cancer [29].

### B. Reproducibility evaluation

Previous studies on breath holding techniques shown the necessity of a good reproducibility and the difficulty to evaluate this reproducibility [22], [31], [21], [1]. This is very important because, by knowing such displacement, it allows to determine IM, and so to evaluate the efficiency of the irradiation with BH compares to FB.

Techniques to assess such reproducibility are 2D or 3D. 2D techniques involves the use of radiographic films [29], [20] or portal images [26], [23]. Evaluation is performed by measuring features such as projection of the top diaphragm cupola [19], [20], [29], [25] relatively to skeleton (assumed to be fixed), or implanted radio-opaque markers [20]. 3D techniques compare several CT scans acquired in equivalent state. Comparisons are made by lung volume differences [1], [31], [21], or lung surface distances [1], [22] (using "A not B; B not A" technique or Distance To Agreement), or features points, such as trachea, carina, center of tumor or diaphragm, which are (mostly manually) localized in each scan [8], [44], [45].

Results are expressed in term of CC, AP, ML displacements for 2D studies, and lung volume percentage difference or mean 3D displacements for 3D studies. Quantification of reproducibility is quite large, from 1.0*mm* [23] to 6.6*mm* [20]. Table VI depicts results of studied evaluating BH interfraction reproducibility, with or without ABC. - VERFIER AVEC TABLEAU DE REMOUCHAMPa PAGE 9

### C. Volume analysis

Patients can be separated in two groups (paired t-test shows the two sets are significantly different), the first (patients $n°1, 2, 5, 6, 7, 8$) with very good lung volume reproducibility and the second (patients $n°3, 4$) with problems.

The first group show comparable results with previous studies (LVD lower than 4.1% or 170*cc* for the whole lung). Hence, Stromberg et al. [31], found mean lung volume differences (in DI) of 4% both for intra and inter session. Wong et al. [1] study intrafraction (30 min apart) varia-

tion of lung volume for three patients and found LVD about 6%. Wilson et al. [21] found inter-fraction LVD from 0.2 to 8.7% ($< 186\,cc$) for right or left lung (differences are not significant, 10 patients). For comparison, if lung were inflating uniformly like a sphere, LVD of 5% for a $5.7L$ volume would lead to a change in the radius of the sphere of $1.8\,mm$ (maximum displacement); the same calculation for a lung of $6.1L$ with a LVD of 16%, lead to $6.3\,mm$.

Two patients have higher differences than previously reported (6 to 16%). Wilson et al. [21] mention one patient with 13.2% ($289cc$) for left lung (authors said difference seems to be due to restitution of lung volume caused by response of tumor to treatment rather than failure of ABC). Analysis for patients $n°3$ shows that the difference is almost equally reported (8.4%) in each lung. Patient $n°4$ shows that most of the difference is localized in the left lung (28% !).

The lung volume increase with BH compare to FB (average 25%) is lower than the ones measured in [4] (average of 42%, range from $23-66\%$), and comparable to the results presented in [8]. It is because all the patients have severe insufficiency respiratory and we use mDIBH rather than DIBH. +++ CAS DE PATIENT 5 AVEC TRES PEU DE INCREASE !!!

### *D. Lung deformation*

We first observe a awaited correlation between the LVD and the mean displacements: when the LVD increase, the mean increase. However, we patient 3 and 5 have similar mean displacement ($4.3mm$) but show different LVD (4.8% vs 8.4%). Standard deviation of displacement is more linearly related to the LVD (reduced chi-square is 1.0, vs 2.0 with mean).

As in [22], we observe less displacement in the upper regions of the lung than in the lower. However, (1) our observed displacement are greater than in [22] and (2) the difference between upper and lower region are also greater (from 1.9 to 4, vs from 1.5 to 2.1, mean left/right). The DTA (Distance To Agreement) between two lung surfaces average the distance of each point of the first lung surface to the closest point in the second surface. Our approach has 2 differences. First, we average distance for each point in the volume (not only on the surface). Second, we compute the distance for an estimation of each point displacement, not its distance to the closest point. It allows to avoid a potential problem with DTA which could tend to underestimate motion (for example in case of vertical sliding motion). It also allows to avoid internal extrapolation needed with surface-based approach.

One important point is the subtraction of the global setup error between the CT acquisitions. Such error is estimated with an automated rigid registration algorithm focusing on the bonny part of the scan. Majority of the patients have very low setup error (lower than $1°$, $2\,mm$), except some scan which was acquired at several days of interval. In some case, we detect setup error up to $30\,mm$.

Two patients have clinical reasons that could explain discrepancies. Patient $n°3$ has an important emphysema bubble of about $512cc$ in the left lung, and numerous other smaller other emphysema bubbles near apex. He moreover has a pleural effusion that increased between acquisitions and right lower lobe atelectasis. OLD ?, VERY TIRED TOO. Patient $n°4$ also has atelectasis and a decreasing pleural effusion. He moreover has a very low forced expiratory volume in the first second (FEV1) of 0.7. Patients with pleural effusion or atelectasis should not be treated with ABC device.

While lung are immobilized, some studies try to evaluate the influence of the heart, because tumor located near the heart my be affected by cardiac motion. [13], [46], [17] think that the heart may not have significant statistical impact on tumor motion. We did not investigate this effect here.

The drawback of the proposed method are the following. Its precision rely on the slice thickness ($5\,mm$ here) which tends to overestimate the displacement in the CC direction. We use linear interpolation throughout the computation, which tends to smooth high gradient. Lower slice thickness ($3\,mm$) or high order interpolation (such as cubic spline) ca improve accuracy. Another drawback is we do not know if an observed displacement comes from a difference of BH or comes from an anatomical changes between the 2 CT scan (tumor regression, ...).

The advantages of the proposed method are the following. It is an automated method. It does not require the determination of corresponding points in each CT scan and so does not rely on the accuracy of such selection. It measure a 3D information in the whole volume: studying the region around the tumor will help to adapt internal margin.

## V. CONCLUSION

BH techniques are promising but reproducibility evaluation is a required first step before allowing to precisely define IM. In this study, we have proposed an original method for 3D interfraction BH reproducibility evaluation. Such method rely on both rigid and non-rigid registration method, allowing to compute the "residual error" which is the 3D displacement of each point of a CT scan. We have reported results on CT scans of patients enrolled in a phase II trial, for which 3 CT scan are acquired in BH with an ABC device. We also have reported lung volume difference analysis and patient compliance.

Active BH with ABC is generally well supported, although patients have severe insufficiency respiratory. For 6 patients, BH is effective and comparable to other interfraction reproducibility studies. The two other patients show insufficient reproducibility and have clinical reasons to explain discrepancies.

3D automated computation tools such as lung volume measurement and deformation field computation presented here allow to perform personalized evaluation of breath hold reproducibility. The drawbacks are the slice thickness leading to potential inaccuracy in the CC direction, the need to acquire several CT scan, the large amount of data to process.

Because such tools lead to a 3D information in each

part of the patient's body, it will be used to adapt internal margin. Such tools can also be used to quantify patient anatomical evolution during the treatment if CT scans are regularly acquired (each week for example). We also plan to use such information to build a patient-adapted 3D breathing model in order to derive 4D dosimetric studies.

## References


[1] JW. Wong, MB. Sharpe, DA. Jaffray, VR. Kini, JM. Robertson, JS. Stromberg, and AA. Martinez. The use of active breathing control (ABC) to reduce margin for breathing motion. *Int J Radiat Oncol Biol Phys*, 44(4):911–19, 1999.

[2] KM. Langen and DT. Jones. Organ motion and its management. *Int J Radiat Oncol Biol Phys*, 50(1):265–78, 2001.

[3] M. Mehta, R. Scrimger, R. Mackie, B. Paliwal, R. Chappell, and J. Fowler. A new approach to dose escalation in non-small-cell lung cancer. *Int J Radiat Oncol Biol Phys*, 49(1):23–33, 2001.

[4] PC. Cheung, KE. Sixel, R. Tirona, and YC. Ung. Reproducibility of lung tumor position and reduction of lung mass within the planning target volume using active breathing control (ABC). *Int J Radiat Oncol Biol Phys*, 57(5):1437–42, 2003.

[5] H.A. Shih, S.B. Jiang, K.M. Aljarrah, K.P. Doppke, and N.C. Choi. Planning target volume determined with fused CT images of fast, breath-hold, and four second simulation ct scans to account for respiratory movement in 3D-CRT in lung cancer. In *ASTRO*, 2002.

[6] K. Tsujino, S. Hirota, M. Endo, K. Obayashi, Y. Kotani, M. Satouchi, T. Kado, and Y. Takada. Predictive value of dose-volume histogram parameters for predicting radiation pneumonitis after concurrent chemoradiation for lung cancer. *Int J Radiat Oncol Biol Phys*, 55(1):110–5, 2003.

[7] Y. Seppenwoolde, K. De Jaeger, and JV. Lebesque. In regard to tsujino et al.: predictive value of dose-volume histogram parameters for predicting radiation pneumonitis after concurrent chemoradiation for lung cancer. *Int J Radiat Oncol Biol Phys*, 56(4):1208–9, 2003.

[8] J. Hanley, MM. Debois, D. Mah, GS. Mageras, A. Raben, K. Rosenzweig, B. Mychalczak, LH. Schwartz, PJ. Gloeggler, W. Lutz, CC. Ling, SA. Leibel, Z. Fuks, and GJ. Kutcher. Deep inspiration breath-hold technique for lung tumors: the potential value of target immobilization and reduced lung density in dose escalation. *Int J Radiat Oncol Biol Phys*, 45(3):603–11, 1999.

[9] K. Yamada, T. Soejima, E. Yoden, T. Maruta, T. Okayama, and K. Sugimura. Improvement of three-dimensional treatment planning models of small lung targets using high-speed multislice computed tomographic imaging. *Int J Radiat Oncol Biol Phys*, 54(4):1210–6, 2002.

[10] T. Neicu, H. Shirato, Y. Seppenwoolde, and SB. Jiang. Synchronized moving aperture radiation therapy (smart): average tumour trajectory for lung patients. *Physics in Medecine and Biology*, 48(5):587–598, 2003.

[11] L. Ekberg, O. Holmberg, L. Wittgren, G. Bjelkengren, and T. Landberg. What margins should be added to the clinical target volume in radiotherapy treatment planning for lung cancer? *Int J Radiat Oncol Biol Phys*, 48(1):71–7, 1998.

[12] C. Ozhasoglu and MJ. Murphy. Issues in respiratory motion compensation during external-beam radiotherapy. *Int J Radiat Oncol Biol Phys*, 52(5):1389–99, 2002.

[13] Y. Seppenwoolde, H. Shirato, K. Kitamura, S. Shimizu, M. van Herk, and JV. Lebesque. Precise and real-time measurement of 3D tumor motion in lung due to breathing and heartbeat, measured during radiotherapy. *Int J Radiat Oncol Biol Phys*, 53(4):822–34, 2002.

[14] S. Essapen, C. Knowles, and D. Tait. Variation in size and position of the planning target volume in the transverse plane owing to respiratory movement during radiotherapy to the lung. *Br J Radiol.*, 74(877):73–6, 2001.

[15] CW. Stevens, RF. Munden, KM. Forster, JF. Kelly, Z. Liao, G. Starkschall, S. Tucker, and R. Komaki. Respiratory-driven lung tumor motion is independent of tumor size, tumor location, and pulmonary function. *Int J Radiat Oncol Biol Phys*, 51(1):62–8, 2001.

[16] P. Giraud, Y. De Rycke, B. Dubray, and et al. Conformal radiotherapy planning for lung cancer: analysis of intrathoracic organ motion during extreme phases of breathing. *Int J Radiat Oncol Biol Phys*, 51(4):1081–1092, 2001.

[17] S. Shimizu, H. Shirato, K. Kagei, and et al. Impact of respiratory movement on the computed tomographic images of small lung tumors in three-dimensional (3D) radiotherapy. *Int J Radiat Oncol Biol Phys*, 46(5):1127–1133, 2000.

[18] EC. Ford, GS. Mageras, E. Yorke, R. Rosenzweig KE, Wagman, and CC. Ling. Evaluation of respiratory movement during gated radiotherapy using film and electronic portal imaging. *Int J Radiat Oncol Biol Phys*, 52(2):522–31, 2002.

[19] R. Wagman, E. Yorke, E. Ford, P. Giraud, G. Mageras, B. Minsky, and K. Rosenzweig. Respiratory gating for liver tumors: use in dose escalation. *Int J Radiat Oncol Biol Phys*, 55(3):659–68, 2003.

[20] LA. Dawson, KK. Brock, S. Kazanjian, D. Fitch, CJ. McGinn, TS. Lawrence, RK. Ten Haken, and J. Balter. The reproducibility of organ position using active breathing control (ABC) during liver radiotherapy. *Int J Radiat Oncol Biol Phys*, 54(1):1410–21, 2001.

[21] EM. Wilson, FJ. Williams, BE. Lyn, JW. Wong, and EG. Aird. Validation of active breathing control in patients with non-small-cell lung cancer to be treated with CHARTWEL. *Int J Radiat Oncol Biol Phys*, 57(3):864–74, 2003.

[22] VM. Remouchamps, N. Letts, D. Yan, FA. Vicini, M. Moreau, JA. Zielinski, J. Liang, LL. Kestin, AA. Martinez, and JW. Wong. Three-dimensional evaluation of intra- and interfraction immobilization of lung and chest wall using active breathing control: a reproducibility study with breast cancer patients. *Int J Radiat Oncol Biol Phys*, 57(4):968–78, 2003.

[23] D. Mah, J. Hanley, KE. Rosenzweig, E. Yorke, CC. Braban L, Ling, SA. Leibel, and G. Mageras. Technical aspects of the deep inspiration breath-hold technique in the treatment of thoracic cancer. *Int J Radiat Oncol Biol Phys*, 48(4):1175–85, 2000.

[24] W.G. O'Dell, M.C. Schell, D. Reynolds, and P. Okunieff. Dose broadening due to target position variability during fractionated breath-held radiation therapy. *Med Phys*, 29(7):1430–1437, 2002.

[25] DJ. Kim, BR. Murray, R. Halperin, and WH. Roa. Held-breath self-gating technique for radiotherapy of non-small-cell lung cancer: A feasibility study. *Int J Radiat Oncol Biol Phys*, 49(1):43–49, 2001.

[26] VM. Remouchamps, N. Letts, FA. Vicini, MB. Sharpe, LL. Kestin, PY. Chen, AA. Martinez, and JW. Wong. Initial clinical experience with moderate deep-inspiration breath hold using an active breathing control device in the treatment of patients with left-sided breast cancer using external beam radiation therapy. *Int J Radiat Oncol Biol Phys*, 56(3):704–15, 2003.

[27] VM. Remouchamps, FA. Vicini, MB. Sharpe, LL. Kestin, AA. Martinez, and JW. Wong. Significant reductions in heart and lung doses using deep inspiration breath hold with active breathing control and intensity-modulated radiation therapy for patients treated with locoregional breast irradiation. *Int J Radiat Oncol Biol Phys*, 55(2):392–406, 2003.

[28] KL. Baglan, MB. Sharpe, D. Jaffray, RC. Frazier, J. Fayad, LL. Kestin, V. Remouchamps, AA. Martinez, J. Wong, and FA. Vicini. Accelerated partial breast irradiation using 3D conformal radiation therapy (3D-CRT). *Int J Radiat Oncol Biol Phys*, 55(2):302–11, 2003.

[29] JM. Balter, KK. Brock, DW. Litzenberg, DL. McShan, TS. Lawrence, R. Ten Haken, CJ. McGinn, KL. Lam, and LA. Dawson. Daily targeting of intrahepatic tumors for radiotherapy. *Int J Radiat Oncol Biol Phys*, 52(1):266–71, 2002.

[30] KE. Sixel, MC. Aznar, and YC. Ung. Deep inspiration breath hold to reduce irradiated heart volume in breast cancer patients. *Int J Radiat Oncol Biol Phys*, 49(1):199–204, 2001.

[31] JS. Stromberg, MB. Sharpe, LH. Kim, VR. Kini, DA. Jaffray, AA. Martinez, and JW. Wong. Active breathing control (ABC) for hodgkin's disease: reduction in normal tissue irradiation with deep inspiration and implications for treatment. *Int J Radiat Oncol Biol Phys*, 48(3):797–806, 2000.

[32] S. Hu, E.A. Hoffman, and J.M. Reinhardt. Automatic lung segmentation for accurate quantitation of volumetric X-ray CT images. *IEEE T Med Im*, 20(6):490–8, 2001.

[33] B. Zitova and J. Flusser. Image registration methods: a survey. *Im. Vis. Comp.*, 21:977–1000, 2003.

[34] F.L. Bookstein. Principal warps: Thin-plate splines and the decomposition of deformations. *IEEE T Pat An Mach Int*, 11:567–585, 1989.

[35] J.P. Thirion. Image matching as a diffusion process: an analogy

with Maxwell's demons. *Medical Image Analysis*, 2(3):243–260, 1998.
[36] P. Cachier and N. Ayache. Regularization in image non-rigid registration: I. trade-off between smoothness and intensity similarity. Technical Report 4188, inria, 2001.
[37] P. Cachier and N. Ayache. Regularization methods in non-rigid registration :ii. isotropic energies, filters and splines. Technical Report 4243, inria, 2001.
[38] S. Clippe V. Boldea, D. Sarrut. Lung deformation estimation with non-rigid registration for radiotherapy treatment. In *MICCAI'2003*, volume 2878, pages 770–7. LNCS, 2003.
[39] B.K.P. Horn and B. Schunk. Determining optical flow. *Artificial Intelligence*, 17:185–203, 1981.
[40] R. Deriche. Recursively implementing the gaussian and its derivatives. Technical Report 1893, INRIA, apr 1993.
[41] M. Bro-Nielsen and C. Gramkow. Fast fluid registration of medical images. In K.H. Hone and R. Kikinis, editors, *vbc*, volume 1131, pages 267–276. lncs, 1996.
[42] F. Maes, A. Collignon, D. Vandermeulen, G. Marchal, and P. Suetens. Multimodality Image Registration by Maximization of Mutual Information. *IEEE T Med Im*, 16(2):187–198, 1997.
[43] W.M. Wells, P.A. Viola, H. Atsumi, S. Nakajima, and R. Kikinis. Multi-Modal Volume Registration by Maximization of Mutual Information. *Medical Image Analysis*, 1(1):35–51, 1996.
[44] H. Onishi, K. Kuriyama, T. Komiyama, S. Tanaka, N. Sano, and Y. Aikawa. A new irradiation system for lung cancer combining linear accelerator, computed tomography, patient self-breath-holding, and patient-directed beam-control without respiratory monitoring devices. *Int J Radiat Oncol Biol Phys*, 56(1):14–20, 2003.
[45] H. Onishi, K. Kuriyama, T. Komiyama, S. Tanaka, J. Ueki, N. Sano, T. Araki, S. Ikenaga, Y. Tateda, and Y. Aikawa. Ct evaluation of patient deep inspiration self-breath-holding: how precisely can patients reproduce the tumor position in the absence of respiratory monitoring devices? *Med Phys*, 30(6):1183–7, 2003.
[46] H. Shirato, S. Shimizu, K. Kitamura, T. Nishioka, K. Kagei, S. Hashimoto, H. Aoyama, T. Kunieda, N. Shinohara, H. Dosaka-Akita, and K. Miyasaka. Four-dimensional treatment planning and fluoroscopic real-time tumor tracking radiotherapy for moving tumor. *Int J Radiat Oncol Biol Phys*, 48(2):435–42, 2000.

## FIGURES

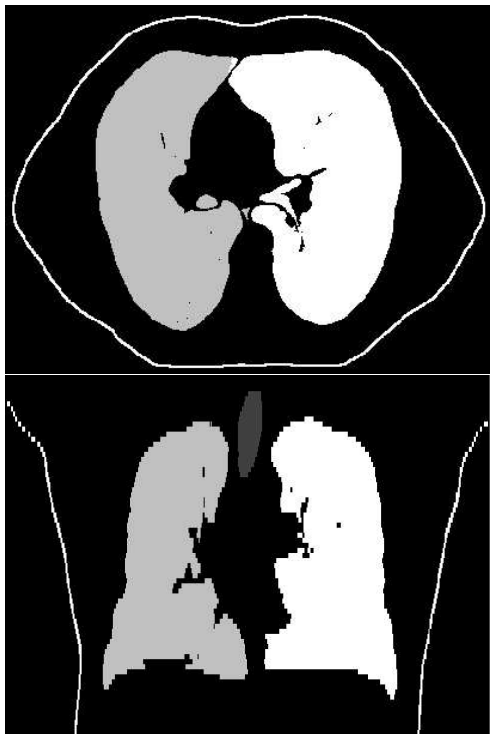

Fig. 1
Slices (axial and coronal) of segmented CT. Trachea, left and right lungs are displayed with different gray levels. Patient boundaries are displayed in white.

| Patient | A-B (cc) | B-C (cc) | A-C (cc) | A-B (%) | B-C (%) | A-C (%) |
|---|---|---|---|---|---|---|
| 1 | 148.6 | 16.5 | 165.1 | 3.9% | 0.4% | 4.1% |
| 2 | 159.5 | 80.8 | 78.7 | 1.8% | 0.9% | 0.9% |
| 3 | 343.2 | 638.8 | 309.9 | 6.6% | 13.1% | 5.6% |
| 4 | 603.4 | 1015.5 | 412.1 | 8.9% | 16.4% | 5.7% |
| 5 | 134.3 | 261.4 | 395.7 | 1.6% | 3.2% | 4.8% |
| 6 | 27.1 | 72.6 | 96.6 | 0.5% | 1.3% | 1.8% |
| 7 | 157.9 | 117.1 | 40.8 | 2.8% | 2.1% | 0.7% |
| 8 | 47.1 | 105.7 | 58.6 | 0.7% | 1.6% | 0.9% |

TABLE I

LUNG VOLUME DIFFERENCES (LVD) FOR THE THREE CT SCANS (DENOTED BY A,B AND C) OF 8 PATIENTS, EXPRESSED IN *cc* AND IN % OF THE FIRST VOLUME. GREY BOXES EMPHASIS LARGE VALUES.

| Patient | Whole lung | | Right lung | | Left lung | |
|---|---|---|---|---|---|---|
| | *cc* | % | *cc* | % | *cc* | % |
| 3 | 431.2 | 8.5% | 284.2 | 8.5% | 146.5 | 8.4% |
| 4 | 698.2 | 10.6% | 196.8 | 4.2% | 506.6 | 28.1% |

TABLE II

LUNG VOLUME DIFFERENCE (LVD) FOR LEFT AND RIGHT LUNG, (IN *cc* AND %) FOR THE THREE PATIENT SHOWING LARGE LVD.

| Patient | FB ($g/cm^3$) | DI ($g/cm^3$) | Vol. % change | Density % change |
|---|---|---|---|---|
| 1 | 0.47 | 0.20 | 20.3% | 33.9% |
| 2 | 0.20 | 0.15 | 25.4% | 5.2% |
| 3 | 0.51 | 0.16 | 18.9% | 42.1% |
| 4 | 0.41 | 0.17 | 7.7% | 28.5% |
| 5 | 0.15 | 0.13 | 15.4% | 1.8% |
| 6 | 0.23 | 0.18 | 34.5% | 6.1% |
| 7 | 0.44 | 0.18 | 19.5% | 32.4% |
| 8 | 0.21 | 0.15 | 32.7% | 6.8% |
| Mean | 0.33 | 0.17 | 21.8% | 19.6% |
| Stdev | 0.15 | 0.02 | 8.8% | 16.2% |
| Mean [8] | 0.26 | 0.19 | n.a. | 26% |
| Stdev [8] | 0.07 | 0.04 | n.a. | 16% |

TABLE III

AVERAGE LUNG DENSITIES FOR THE 8 PATIENTS MEASURED FROM THE FB AND DI CT SCANS.

| Patient | Mean (mm) | Median (mm) | Std dev (mm) | 5% max (mm) |
|---|---|---|---|---|
| 1 | 3.4 | 2.9 | 2.0 | 9.0 |
| 2 | 2.3 | 1.9 | 1.4 | 6.2 |
| 3 | 4.3 | 3.3 | 3.3 | 13.7 |
| 4 | 6.8 | 5.2 | 5.1 | 21.9 |
| 5 | 4.7 | 4.2 | 2.5 | 11.0 |
| 6 | 2.8 | 2.3 | 1.8 | 7.4 |
| 7 | 2.3 | 1.8 | 1.7 | 7.0 |
| 8 | 2.7 | 2.3 | 1.5 | 6.4 |

TABLE IV

MEAN, MEDIAN, STANDARD DEVIATION OF NORM OF THE DISPLACEMENTS FOR ALL POINTS INSIDE LUNG (FROM 870 000 UP TO 2 MILLIONS OF POINTS ACCORDING TO THE PATIENT). FOURTH COLUMN INDICATES MEAN OF THE 5% OF POINTS HAVING GREATER DISPLACEMENT. EACH COMPUTATION IS AVERAGED OVER 6 VECTOR FIELDS.

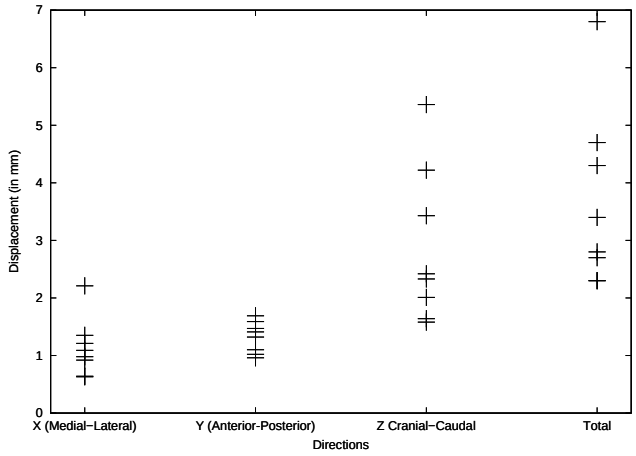


Fig. 2

Mean points displacements (in mm) for each patient, in the three directions X (Lateral), Y (AnteriorPosterior), Z (Cranio-Caudal) and the 3D norm.

| Distance | p°1, 2, 5, 6, 7, 8 | | p°3, 4 | | [22] | |
|---|---|---|---|---|---|---|
| | left | right | left | right | left | right |
| Volume | | | | | | |
| 1 (superior 10%) | 2.0(0.7) | 1.8(0.7) | 2.7(1.0) | 2.4(0.8) | | |
| 2 (next 20%) | 2.7(1.7) | 2.1(1.0) | 3.9(2.0) | 3.1(1.6) | | |
| 3 (next 20%) | 2.7(1.3) | 2.5(1.3) | 6.1(3.4) | 4.2(2.3) | | |
| 4 (next 20%) | 3.2(1.6) | 3.0(1.6) | 7.9(4.1) | 4.8(2.8) | | |
| 5 (next 20%) | 3.9(2.0) | 3.7(1.8) | 8.1(4.5) | 8.2(4.5) | | |
| 6 (inferior 10%) | 4.1(1.9) | 4.0(1.6) | 8.5(3.5) | 9.4(4.2) | | |
| Surface | | | | | | |
| 1 (superior 10%) | 2.0(0.8) | 1.9(0.8) | 2.7(1.2) | 2.3(0.9) | 1.6(1.1) | 1.4(1.2) |
| 2 (next 20%) | 2.6(1.7) | 2.2(1.1) | 3.8(2.1) | 2.9(2.1) | 1.1(1.1) | 1.2(1.1) |
| 3 (next 20%) | 2.5(1.2) | 2.4(1.3) | 6.1(3.6) | 4.3(3.1) | 1.0(1.1) | 1.0(1.1) |
| 4 (next 20%) | 2.7(1.5) | 2.8(1.6) | 7.6(4.2) | 4.3(3.2) | 1.1(1.2) | 1.3(1.3) |
| 5 (next 20%) | 3.4(1.9) | 3.5(1.9) | 8.0(4.7) | 6.1(4.5) | 1.9(2.2) | 1.7(1.9) |
| 6 (inferior 10%) | 3.9(2.1) | 4.1(1.8) | 8.2(3.5) | 8.2(4.5) | 2.1(2.1) | 2.0(1.8) |

TABLE V

Mean points displacements (in mm) for six successive regions normalized to the left and right lung height (superior 10%, four successive 20% and inferior 10%), averaged for patients n°1, 2, 5, 6, 7, 8, patients n°3, 4 and compared to result of [22]).
MANQUE DTA !!!

Fig. 3
Example of the projection of 3D vectors (sampled each $4\,mm$ for visual purpose) on three slices. Each point displacement is depicted with an red vector ended by a green arrow.

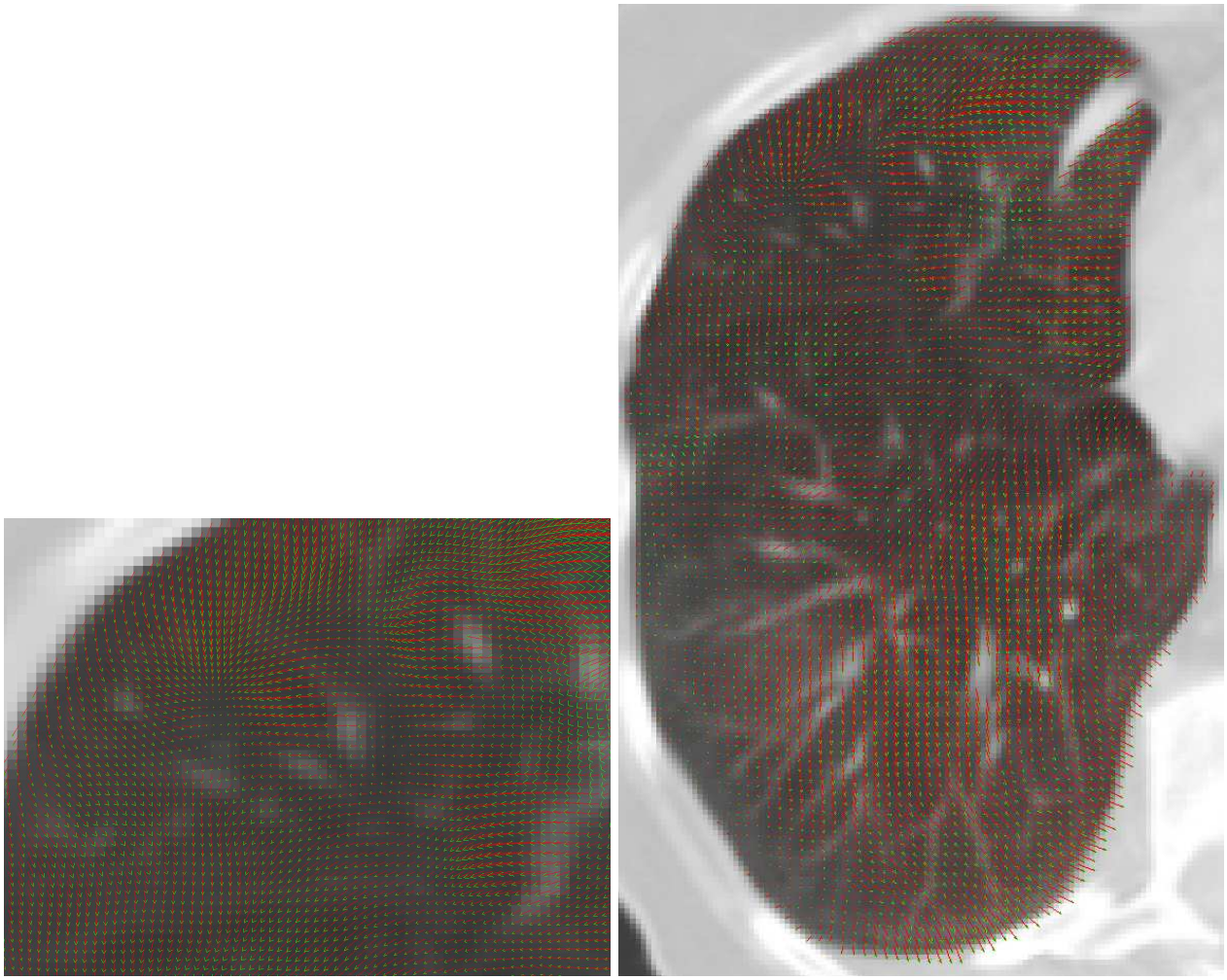

Fig. 4
Closeup on the previous vectors fields.

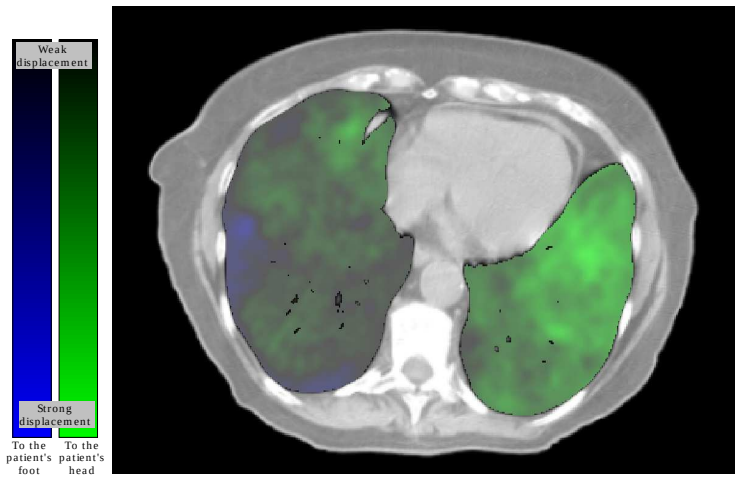


Fig. 5

Cranio-Caudal displacement on an axial slice. Green represent displacements to patient's head and blue represents displacements to patient's foot.


Fig. 6

Norm of 3D vectors on an axial slice. Dark red represents higer norm, light red represents lower norm.

| *Ref* | *Date* | *mm (stdev)* | *features* | *Active/Level* | *2D/3D* | *cancer* | *method* |
|---|---|---|---|---|---|---|---|
| remouchamps2003b | 2003 | CC=3.2 ML=2.4 rot=1° | median beam | ABC mDIBH | 2D | breast | 509 EPID, 5 patients |
| | | CC=3.1 ML=2.3 rot=1° | lateral beam | | | | skin tatoo (for setup), isocenter and field border for EPID |
| balter2002 | 2002 | AP=2.3 ; ML=2.1 | skeleton | ABC NE | 2D | liver | CT/Film comparisons, Radiographs, rel to skel or diaph, liver, Xray brain lab 8 patients |
| | | CC=2.5 | diaphragm | | | | radiographs |
| dawson2001 | 2001 | CC=6.6 ; AP=3.2 ; ML=3.2 | Hepatic microcoils | ABC NE | 2D | liver | Radiographs, rel. to skel |
| | | CC=4.4 | diaphragm | | | | Rel to skel, radiographs, include microcoils, 262 fractions (8patients) |
| kim2001 | 2001 | CC<5 | diaphragm | Self NE/NI DE/DI | 2D | NSCLC | 16 patients, Fluoro, film + video |
| mah2000 | 2000 | from -12 to 11 / 1.3(5.3) range=9.1 | diaphragm | Self DI | 2D | NSCLC | diaphg rel. to isocenter, 92 portal film, 7 patients (250 ttt) sur 16 (400ttt effectués) |
| | | 0.2 (1.4) | GTV center | | | | |
| hanley1999 | 1999 | 2.5(1.6) | diaphragm | Self DI | 2D | NSCLC | 5 patients, fluoro |
| cheung2003 | 2003 | CC=1.1(3.5) AP=1.2(2.3); ML=0.3(1.8) | GTV center | ABC DI | 3D | NSCLC | 10 patients, 5CT par patient (que 8 avec les 5CT) |
| onishi2003a | 2003 | CC: 2.2(1.1) AP: 1.4(0.6)ML: 1.3(0.5) | Tumor | Self DI | 3D | NSCLC | 20 patients, 3CT |
| remouchamps2003a | 2003 | 1.4(1.7) | Lung surface | ABC mDIBH | 3D | breast | DTA 30 patients, 2 CT (que 14 ont 2 CT ?) |
| | | 1.4(1.0) | Trachea | | | | |
| | | 1.9 (2.2) | diaphragm | | | | |
| onishi2003b | 2003 | CC=2.1 AP=1.4 ML=1.3 | Tumor (active mode) | Self DI | 3D | lung | Self mais passive=ordre par phys et active= choix BH par patient |
| | | CC=3.1 AP=2.4 ML=2.2 | Tumor (passive mode) | | | | 3CT actif + 3 CT passif |
| wilson2003 | 2003 | 0.2 to 8.7 %, max=13.2% | lung volume | ABC mDIBH | 3D | NSCLC | 11 patient, 1FB + 3 CT (warning ! def intra/inter ) |
| stromberg2000 | 2000 | 4.0% | lung volume | ABC DI | 3D | Hodgkin | 5 patients, 5CT (NE,NI,3DI) |
| wong99ABC | 1999 | 6.0% | lung volume | ABC NE / DI | 3D | lung, liver, | intrafraction !!!!! |
| hanley1999 | 1999 | lat width=1.1%; AP height=1.5% | overlapping sclices | Self DI | 3D | NSCLC | 5 patients, 4CT (que 3p), 2CT sinon |
| | | lung area = 3% | | | | | |

TABLE VI

Review of interfraction reproducibility studies